An Unbiased Evaluation of CK2 Inhibitors by Chemoproteomics

CHARACTERIZATION OF INHIBITOR EFFECTS ON CK2 AND IDENTIFICATION OF NOVEL INHIBITOR TARGETS*[S]

James S. Duncan‡§, Laszlo Gyenis‡, John Lenehan‡, Maria Bretner¶‖, Lee M. Graves, Timothy A. Haystead‡‡, and David W. Litchfield‡§§**

Recently protein kinases have emerged as some of the most promising drug targets; and therefore, pharmaceutical strategies have been developed to inhibit kinases in the treatment of a variety of diseases. CK2 is a serine/threonine-protein kinase that has been implicated in a number of cellular processes, including maintenance of cell viability, protection of cells from apoptosis, and tumorigenesis. Elevated CK2 activity has been established in a number of cancers where it was shown to promote tumorigenesis via the regulation of the activity of various oncogenes and tumor suppressor proteins. Consequently the development of CK2 inhibitors has been ongoing in preclinical studies, resulting in the generation of a number of CK2-directed compounds. In the present study, an unbiased evaluation of CK2 inhibitors 4,5,6,7-tetrabromo-1*H*-benzotriazole (TBB), 4,5,6,7-tetrabromo-1*H*-benzimidazole (TBBz), and 2-dimethylamino-4,5,6,7-tetrabromo-1*H*-benzimidazole (DMAT) was carried out to elucidate the mechanism of action as well as inhibitor specificity of these compounds. Utilizing a chemoproteomics approach in conjunction with inhibitor-resistant mutant studies, CK2α and CK2α' were identified as *bona fide* targets of TBB, TBBz, and DMAT in cells. However, inhibitor-specific cellular effects were observed indicating that the structurally related compounds had unique biological properties, suggesting differences in inhibitor specificity. Rescue experiments utilizing inhibitor-resistant CK2 mutants were unable to rescue the apoptosis associated with TBBz and DMAT treatment, suggesting the inhibitors had off-target effects. Exploitation of an unbiased chemoproteomics approach revealed a number of putative off-target inhibitor interactions, including the discovery of a novel TBBz and DMAT (but not TBB) target, the detoxification enzyme quinone reductase 2 (QR2). The results described in the present study provide insight into the molecular mechanism of action of the inhibitors as well as drug specificity that will assist in the development of more specific next generation CK2 inhibitors. ***Molecular & Cellular Proteomics 7:1077–1088, 2008.***

Targeting protein kinases for therapeutic applications has become a rapidly evolving field with a number of successful inhibitors in clinical studies or approved for treatment of various cancers. Loss of regulation of protein kinase activity has been identified as a key event in the development of cancer and has therefore become an avenue of intense research. Specifically the success of targeted therapies such as Gleevec (imatinib) for the treatment of chronic myelogenous leukemia has provided a model for the development of novel inhibitors targeting a wide variety of protein kinases (1). Recently protein kinases have emerged as some of the most promising drug targets, representing as much as 20% of the "druggable" genome (2, 3). Ongoing preclinical studies targeting serine/threonine kinases have been carried out demonstrating the potential of kinase inhibitors as anticancer therapeutics, including the study of protein kinase CK2.

CK2 (formally known as casein kinase II) is a ubiquitously distributed, constitutively active serine/threonine kinase implicated in multiple cellular processes, including cell survival, protection of cells from apoptosis, and tumorigenesis (4). Elevated CK2 activity has been documented in a number of cancers where high CK2 activity has been correlated with aggressive tumor behavior (5). Detailed studies have been carried out to elucidate the molecular mechanism of CK2 in tumorigenesis, demonstrating that increased CK2 activity promotes a number of pathways participating in the development of cancer (6, 7). Proposed modes of action of CK2 in tumorigenesis are through the regulation of key oncogenes and tumor suppressor proteins within various prosurvival pathways including the Wnt (8), nuclear factor-κB (9), and phosphatidylinositol 3-kinase pathways (10). Regulation of oncogene and tumor suppressor proteins by CK2 phosphorylation has been shown to influence susceptibility to proteosome degradation, protect proteins from caspase-mediated cleavage, and alter the protein activity (11). Taken together, elevated CK2 activity promotes a prosurvival signal in cancer by facilitating the transcription, activation, or stability of on-

From the ‡Department of Biochemistry, The University of Western Ontario, London, Ontario N6A 5C1, Canada, ¶Institute of Biochemistry and Biophysics, Polish Academy of Sciences, 5a Pawińskiego St., 02-106 Warszawa, Poland, **Department of Pharmacology, University of North Carolina, Chapel Hill, North Carolina 27599-7365, and ‡‡Department of Pharmacology, Duke University Medical Center, Durham, North Carolina 27710

Received, November 26, 2007, and in revised form, January 22, 2008

Published, MCP Papers in Press, February 7, 2008, DOI 10.1074/mcp.M700559-MCP200

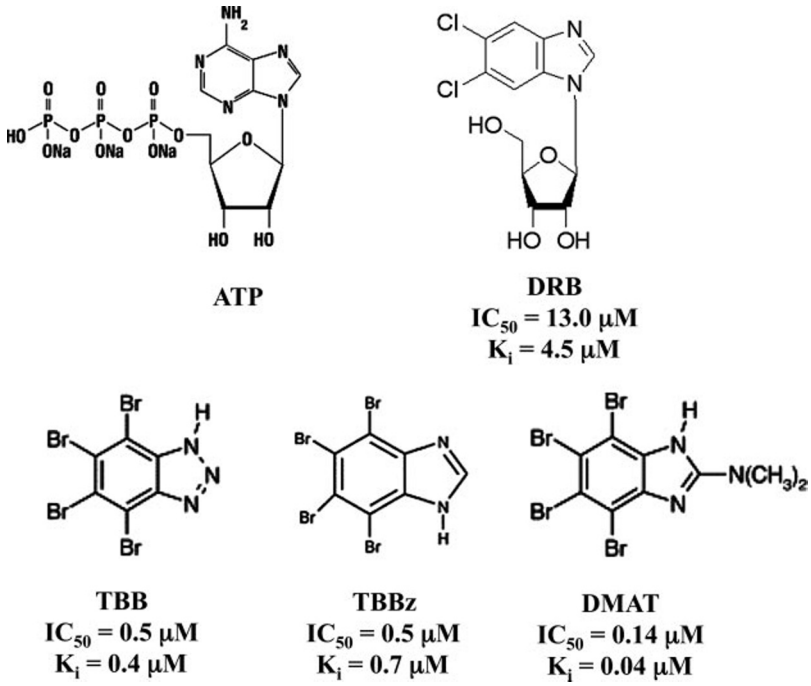

FIG. 1. **Chemical structure of ATP and commercially available CK2 inhibitors.** IC_{50} and K_i values are in μM concentrations. *DRB*, 5,6-dichlorobenzimidazole ribofuranoside.

cogenes and antiapoptotic proteins while repressing tumor suppressor activity through increased proteosome degradation. Recently an antiapoptotic role of CK2 has emerged as a number of substrates were identified that exhibited protection from caspase cleavage following CK2 phosphorylation (12–16). Consequently CK2 has emerged as a promising target for therapeutic intervention in the treatment of cancer.

Development of specific ATP-competitive protein kinase inhibitors has been historically difficult as many cellular proteins utilize ATP as a substrate; however, exploitation of unique structural aspects of kinases has provided an avenue to develop highly selective inhibitors. A number of ATP-competitive inhibitors have been developed to target CK2 based on the solved crystal structure, which shows unique structural properties that distinguish CK2 from the majority of other kinases (17). Most notably, CK2 was found to have a relatively small ATP binding pocket, compared with other protein kinases, due to the presence of large bulky residues that are essential for ATP binding. Exploitation of these distinctive bulky residues within the ATP binding pocket has provided opportunities to develop highly selective CK2 inhibitors. Based on the structure of a known CK2 inhibitor, 5,6-dichlorobenzimidazole ribofuranoside, a novel compound 4,5,6,7-tetrabromo-1*H*-benzotriazole (TBB)[1] was engineered (18) that displayed a high affinity for CK2 due to strong hydrophobic and Van der Waals interactions with the large bulky residues in the ATP binding pocket (Fig. 1). TBB exhibited high selectivity for CK2 in a panel of 30 kinases; however, there were a handful of kinases that were sensitive to the inhibitors, including DYRK1a (dual specificity tyrosine phosphorylation-regulated kinase 1a), which was inhibited to nearly the same extent as CK2, whereas glycogen synthase kinase β, CDK2, and phosphorylase kinase were inhibited to a lesser extent. Therefore, strategies to improve the selectivity of the inhibitors were undertaken focusing on generating compounds that had improved interaction with the unique bulky residues. Utilizing the TBB backbone as a scaffold, two next generation derivatives were engineered, 4,5,6,7-tetrabromo-1*H*-benzimidazole (TBBz) and 2-dimethylamino-4,5,6,7-tetrabromo-1*H*-benzimidazole (DMAT) (19, 20). *In vitro* studies testing the efficacy of DMAT showed that substitution of the imidazole ring and the addition of bulky constituents resulted in a higher affinity and selectivity toward CK2 with a K_i value of 40 nM.

In this study, an unbiased evaluation of TBB and related CK2 inhibitors utilizing chemoproteomics was carried out to investigate the potential of the inhibitors as anticancer therapeutics. A detailed study of the specificity of the CK2 inhibitors TBB, TBBz, and DMAT for CK2 as well as the cellular effects associated with each inhibitor was carried out. Differences between inhibitors in the induction of apoptosis were observed following treatment of HeLa cells with TBB, TBBz, or DMAT, indicating that the inhibitors have unique biological properties as well as revealing the potential for off-target effects. Therefore, rescue experiments utilizing inhibitor-resistant CK2 mutants were used to investigate the specificity of

[1] The abbreviations used are: TBB, 4,5,6,7-tetrabromo-1*H*-benzotriazole; TBBz, 4,5,6,7-tetrabromo-1*H*-benzimidazole; DMAT, 2-dimethylamino-4,5,6,7-tetrabromo-1*H*-benzimidazole; PBST, PBS with Tween 20; TBST, TBS with Tween 20; HA, hemagglutinin; PARP, poly(ADP-ribose) polymerase; HRP, horseradish peroxidase; 2D, two-dimensional; ANOVA, analysis of variance; FACS, fluorescence-activated cell sorting; QR2, quinone reductase 2.

the inhibitors, particularly whether the apoptosis associated with drug treatment was CK2-dependent. The inability to rescue TBBz- and DMAT-induced apoptosis with the resistant mutants prompted a systematic characterization of inhibitor protein targets utilizing a chemoproteomics approach.

MATERIALS AND METHODS

Cell Culture and Transfections—HeLa and U2OS cells were cultured in Dulbecco's modified Eagle's medium (Invitrogen) containing 10% fetal bovine serum (Invitrogen), 100 units/ml penicillin, and 100 μg/ml streptomycin (Invitrogen) on 10- or 15-cm plates (Falcon). HeLa and U2OS cells were transfected with either wild type CK2α/α′, inhibitor-resistant CK2αR/α′R, or kinase-inactive CK2α′-KD in addition to CK2β/CK2β6KR using calcium phosphate with a transfection efficiency of >80%. Cells were treated with TBB (Calbiochem), TBBz (Sigma), or DMAT (Calbiochem) at a final concentration of 8–25 μM for 6, 12, 18, and 24 h. Microscopy images were captured on an inverted microscope (Axiovert S25, Zeiss) using a mounted digital camera (QiCAM, QImaging). HeLa S3 suspension cells were cultured in minimum Eagle's medium (Sigma) containing 10% fetal bovine serum (Invitrogen), 100 units/ml penicillin, and 100 μg/ml streptomycin. Cells were grown to confluency and harvested for use in chemoproteomics experiments.

Cloning of CK2αR and CK2α′R—Inhibitor-resistant CK2 mutants were engineered using a QuikChange II site-directed mutagenesis kit (Stratagene). Human CK2α-HA pRc/CMV was PCR-amplified to make the V66A mutation (mutations are shown in bold) using the primer 5′-GAAAAAGTT**GCA**GTTAAAATTC-3′ and the I174A mutation using 5′-GCTACGACTA**GCA**GACTGGGGTTTGGC-3′. Human HA-CK2α′ pRc/CMV was PCR-amplified to make the V67A mutation using the primer 5′-ATGAGAGAGTG**GCT**GTAAAAATCCTGA-3′ and the I175A mutation using 5′-AAGCTGCGACTG**GCA**GATTGGGGTCTG-3′.

Flow Cytometry—HeLa cells were trypsinized at 18 h following treatment with 8 or 25 μM CK2 inhibitors. Cells were washed in ice-cold PBS and filtered using a cell strainer (VWR) to obtain single cell suspensions. Cells were fixed by the addition of ice-cold 95% ethanol and stored at −20 °C. Cells were then washed in PBS, and the DNA was stained with PI staining solution (50 μg/ml propidium iodide (Sigma), 0.1% sodium citrate, 0.1% Triton X-100, and 100 μg/ml RNase A) in the dark for 1 h at 37 °C. Cells were diluted with PBS to 1 ml and analyzed by flow cytometry (FACSCalibur). Spectra and statistics representing the amount of DNA in different cell cycle stages were prepared using FlowJo flow cytometry analysis software.

Western Analysis—HeLa and U2OS cells were harvested from 10- and 15-cm plates (Falcon) in lysis buffer containing 20 mM Tris (pH 7.5), 150 mM NaCl, 1 mM EDTA, 1 mM EGTA, 1.0% Triton-X-100, 0.5% Nonidet P-40, 2.5 mM sodium pyrophosphate, 1 mM Na_3VO_4, 1 mg/ml leupeptin, and 1 mM PMSF. Lysates were sonicated, and protein concentrations were determined by BCA assay. Proteins were resolved by 12% SDS-PAGE followed by transfer to PVDF membranes (Roche Applied Science). Membranes were blocked with 5% BSA, PBST; 5% BSA, TBST; or 5% nonfat milk, TBST for 1 h followed by an overnight incubation at 4 °C with the primary antibody in 5% BSA, TBST or 5% nonfat milk, TBST. Membranes were probed with primary antibodies including: anti-poly(ADP-ribose) polymerase (PARP) (1:1000) (Cell Signaling Technologies), anti-HA 3F10 (1:100) (Roche Applied Science); anti-c-Myc 9E10 (1:10,000) (Berkeley Antibody Co.), β-tubulin (1:100) (Sigma); HSP90 (1:5000) (Santa Cruz Biotechnology), anti-CK2α (1:5000) polyclonal antiserum directed against the C-terminal synthetic peptide α-(376–391), and anti-CK2α′ (1:5000) polyclonal antiserum directed against the C-terminal synthetic peptide α′-(333–350). Membranes were washed with PBST or TBST and then incubated with appropriate secondary antibodies including: HRP-conjugated goat anti-rabbit (Bio-Rad) (1:2000 for PARP and 1:25,000 for HSP90, CK2α, and CK2α′ antibodies), HRP-conjugated goat anti-mouse (Bio-Rad) (1:1000 for β-tubulin), and HRP-biotin (Jackson ImmunoResearch Laboratories) (1:10,000 for HA 3F10 and c-Myc 9E10). Following secondary antibody incubation, membranes were washed with PBST or TBST and visualized by ECL (Amersham Biosciences). X-ray film (Eastman Kodak Co.) was developed and converted to a digital image using a CanoScan N650U/N656U scanner. Images were visualized in Adobe Photoshop CS.

Immunoprecipitations—HeLa cells were co-transfected with wild type CK2α-HA or inhibitor-resistant CK2αR-HA, myc-CK2β, and EGFP-C2 using calcium phosphate with a transfection efficiency of >80%. Following transfection, cells were treated with DMSO and 8 μM TBB, TBBz, or DMAT for 18 h. To test the ability of CK2α′R to rescue inhibitor-dependent changes, U2OS cells were co-transfected with HA-CK2α′-wt or HA-CK2αR and myc-CK2β and then treated with 25 μM DMSO or DMAT for 12 h. Cell lysates were prepared in RIPA lysis buffer (150 mM NaCl, 50 mM Tris (pH 7.5), 1% Nonidet P-40, 0.5% deoxycholic acid, 0.1% SDS, and 1 mM EDTA), and the protein concentration was determined by BCA assay (Pierce). Equal amounts of protein were incubated with 20 μl of 50% protein A-Sepharose beads (Amersham Biosciences) and 1–5 μg of 12CA5 HA antibody (Roche Applied Science). Following a 1-h incubation tumbling at 4 °C, protein A-Sepharose beads were isolated by centrifugation and washed extensively. Beads were then incubated in SDS loading buffer, boiled for 5 min, and centrifuged briefly to remove beads. Proteins were resolved by 12% SDS-PAGE and transferred to a PVDF membrane followed by Western blot analysis. Membranes were probed with biotinylated anti-HA 3F10 and anti-c-Myc 9E10 antibodies.

ATP-Sepharose Affinity Chromatography—HeLa S3 cells cultured in 1-liter spinner flasks were lysed in buffer A (150 mM NaCl, 50 mM HEPES, 10 mM $MgCl_2$, 1% Nonidet P-40, 1 μg/ml leupeptin, 1 μg/ml aprotinin, and 1 mM dithiothreitol) and incubated on ice for 10 min. Lysates were sonicated and subjected to centrifugation at 80,000 × *g* for 30 min at 4 °C. Equal volumes of lysates were incubated with DMSO and either 1 μM TBBz or 100 μM TBB, TBBz, or DMAT for 2 h with gently rocking at 4 °C. ATP-Sepharose beads (as described earlier (21)) were then added to the lysates containing the inhibitors and incubated at 4 °C for 15 min to allow for binding. ATP-Sepharose beads were isolated by centrifugation and washed extensively with 100 column volumes of buffer A followed by a wash with 1 M NaCl buffer A, and finally beads were equilibrated with buffer A. Equilibrated ATP-Sepharose beads were then incubated in 2D lysis buffer for 15 min with gentle rocking at 4 °C. Protein concentrations were determined by Bradford assay. Equal concentrations of protein from each treatment were resolved by one-dimensional and 2D gel electrophoresis.

2D Gel Electrophoresis—Following inhibitor treatment, cells were harvested from 15-cm plates using PBS-EDTA and collected by centrifugation. Proteins were purified via TRIzol extraction according to Lysis and Protein Extraction from ^{32}P-Labeled WEHI Cells with TRIzol Isolation Reagent, AfCS Procedure Protocol ID PP00000155. Purified proteins were resuspended in 2D lysis buffer containing 7 M urea, 2 M thiourea, 4% (w/v) CHAPS, 1 mM benzamidine, 2.5 mg/ml leupeptin, 20 μg/ml pepstatin, 10 μg/ml aprotinin, 1 mM DTT, 200 mM Na_3VO_4, 100 μM microcystin, and 0.5% (v/v) Ampholines pI 4–7 buffer (Amersham Biosciences). Protein concentrations were determined by Bradford assay (Bio-Rad). Protein samples (150–250 μg) were mixed with rehydration buffer containing 7 M urea, 2 M thiourea, 4% CHAPS, 50 mM DTT, 0.5% Ampholines, and bromphenol blue and then applied to

Immobiline Dry strips (Amersham Biosciences) (7 cm, pI 4–7 or 13 cm, pI 3–10) in ceramic strip holders (Amersham Biosciences). The first dimension isoelectric focusing was carried out using the IPGphor II (Amersham Biosciences) using the following program for the 7-cm IPG strips: rehydration step 1, 20 V for 12 h at 20 °C; step 2, 100 V for 100 V-h; step 3, 500 V for 500 V-h; step 4, 1000 V for 1000 V-h; step 5, 2000 V for 2000 V-h; step 6, 4000 V for 4000 V-h; and step 7, 8000 V for 16,000 V-h. The following program was used for the 13-cm strip: rehydration step 1, 20 V for 12 h at 20 °C; step 2, 100 V for 2 h; step 3, 500 V for 500 V-h; step 4, 1000 V for 1000 V-h; step 5, 2000 V for 4000 V-h; step 6, 4000 V for 8000 V-h; step 7, 6000 V for 12,000 V-h; and step 8, 8000 V for 64,000 V-h. The IPG strips were then incubated in equilibration buffer containing 10 mg/ml DTT (Sigma) followed by 25 mg/ml iodoacetamide (Sigma). The 7-cm IPG strips were then applied to a 12% SDS-polyacrylamide gel, sealed with 0.5% agarose gel, and run at 200 V for 1 h (Bio-Rad Mini-Protean 3 Dodeca Cell), whereas the 13-cm IPG strips were run on 10% SDS-polyacrylamide gels (Hoefer Inc. instruments). Following protein separation, gels were fixed and stained with SYPRO Ruby (Invitrogen) overnight at room temperature. Stained gels were washed and imaged using the ProXPRESS 2D Proteomic Imaging System (PerkinElmer Life Sciences).

2D Gel Electrophoresis Quantification and Analysis—Differences in protein spots between 2D gels were analyzed utilizing Phoretix 2D evolution software (TT900 S2S and PG220, Nonlinear Dynamics). Four gel images from each treatment were imported into Phoretix software, and spots were aligned using SameSpot TT900 S2S same spot analysis. The aligned images were then imported into Progenesis PG220 software for analysis of spot differences and spot intensity. Spot filtering was applied to all aligned gels to normalize for pixel intensity and area with a normalized volume value of >0.005. Statistical analysis of spot changes were performed using ANOVA, and the means were compared with a *t* test where $p = 0.05$.

Sample Preparation and Mass Spectrometry—Following staining of 2D gels with SYPRO Ruby and identification of spot differences using Phoretix Evolution, spots were picked from gels manually or by the Ettan Spot Picker (Amersham Biosciences) and suspended in 50% methanol and 5% acetic acid. Trypsin digestion was performed on excised spots using the MassPREP automated digester (Waters). Peptides were lyophilized, suspended in 30% ACN, 0.1% TFA mixed with α-cyano-4-hydroxycinnamic acid in 50% ACN, 50% 25 mM ammonium citrate, 0.1% TFA and analyzed by MALDI MS and/or MS/MS on the 4700 proteomics analysis MALDI (TOF/TOF) instrument (Applied Biosystems). MS and/or MS/MS analysis was carried out with an *m/z* range of 800–4000 Da and mass tolerance of 50 ppm with a resolution of ~15,000. Peptide fingerprinting was evaluated using GPS Explorer work station version 3.0 series (Applied Biosystems) in conjunction with MASCOT using an internal calibration with a minimum signal-to-noise threshold of 20, a peptide mass exclusion tolerance of 50 ppm, five minimum peaks to match, and a maximum outlier error of 15 ppm with no more than one missed cleavage. Peptide standards consisted of des-Arg-bradykinin (904.468), angiotensin 1 (1296.685), Glu^1-fibrinopeptide (1570.677), ACTH-(1–17) (2093.087), and ACTH-(18–39) (2465.199); the mass exclusion list consisted of 842.5099, 870.509, and 2211.1096. Peptides were searched against the human Swiss-Prot database (release 54.0; July 24, 2007; 276,256 sequence entries) with oxidation as a variable modification (Met).

RESULTS

Effect of CK2 Inhibitors on Cell Viability: Evidence for Unique Modes of Drug Action

Pharmacological inhibition of CK2 has been shown to sensitize various cancer cell lines to apoptosis as well as induce apoptosis directly (19, 22–24). A number of highly specific chemical compounds have been developed to target CK2 in cells including TBB and its derivatives, TBBz and DMAT. To further characterize the effect of these TBB-derived inhibitors on cancer cell viability, an evaluation of inhibitor-induced apoptosis was performed utilizing HeLa cells (Fig. 2*A*). The cleavage of PARP was used as a biological marker of apoptosis and caspase activation. Etoposide, a known apoptotic stimulus, was used as a positive control, whereas DMSO, the drug carrier for all the inhibitors being investigated, was used as a negative control. Induction of apoptosis was evident by the production of cleaved PARP following 24 h of treatment with 25 μM etoposide, TBB, TBBz, and DMAT. Interestingly the induction of apoptosis was observed following 12 h of treatment with TBBz and DMAT but not until 24 h following treatment with the same concentration of TBB. It appears that the different derivatives have varying abilities to induce apoptosis at the same concentration where TBBz and DMAT were the most potent inhibitors. The induction of apoptosis by TBBz and DMAT was further investigated, revealing a dose-dependent effect in which increasing drug concentration resulted in a more potent apoptotic response as is evident by an amplified cleavage of PARP (supplemental material).

To further characterize the biological responses of cells treated with CK2 inhibitors TBB, TBBz, and DMAT, we examined changes in protein profiles using 2D gel electrophoresis. HeLa cells were treated with 25 μM TBB, DMAT, TBBz, or DMSO for 12 h and subjected to 2D gel electrophoresis, and the resultant spot changes were analyzed using 2D Phoretix software. Spots with differences between treatments were identified (spots 1–4), excised from the gels, and subjected to mass spectrometry for protein identification. Spot 1 (~48 kDa), spot 2 (~45 kDa), and spot 3 (~25 kDa) were identified in the TBBz and DMAT (but not in TBB or DMSO) gels as Vimentin proteolytic products by MS analysis (Fig. 2*B*). The fragments generated were consistent with previous findings demonstrating a caspase-dependent apoptosis where Vimentin (57 kDa) was found to be cleaved by caspases 3, 6, and 7 into fragments with molecular masses of 48, 45, and 25 kDa (25). Keratin 18 was also identified as a proteolytic fragment (spot 4, ~22 kDa) present in the TBBz-and DMAT-treated (but not TBB- or DMSO-treated) gels by MS analysis. The cleavage of Keratin 18 (48 kDa) by caspases 3, 6, and 7 during apoptosis has been shown in previous studies and results in the generation of proteolytic fragments, including a 22-kDa peptide (26). Overall an analysis of the proteome of TBBz- and DMAT-treated HeLa cells provided further evidence for inhibitor-dependent apoptosis as well as suggested that the apoptosis stimulated by TBBz and DMAT was mechanistically similar, requiring caspase activation. The potent induction of apoptosis following TBBz and DMAT treatment suggests a unique mechanism of action relative to TBB.

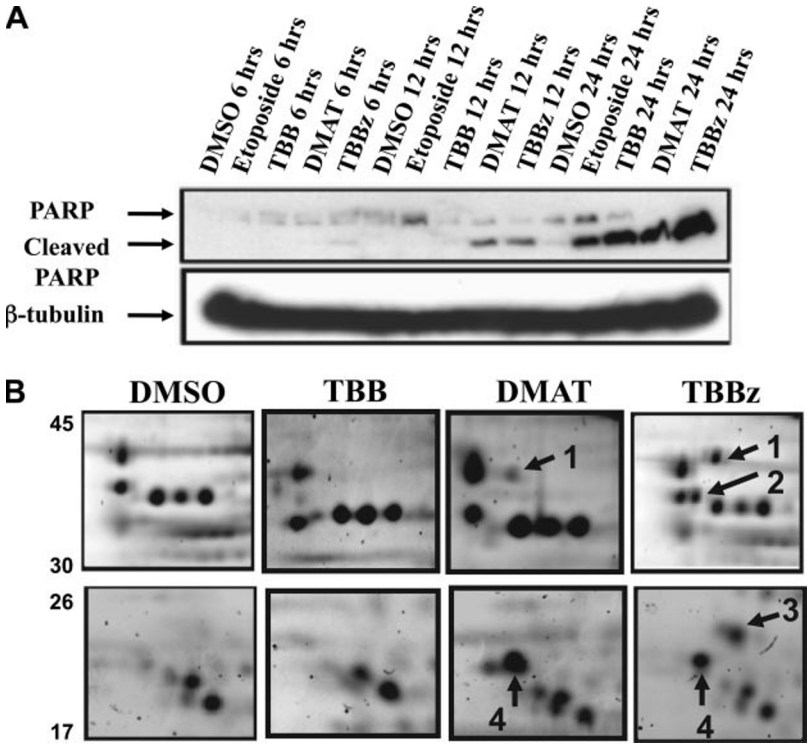

FIG. 2. **CK2 inhibitor-dependent induction of caspase-mediated apoptosis.** *A*, HeLa cells treated with DMSO and either 25 μM etoposide, TBB, DMAT, or TBBz for 6, 12, and 24 h were harvested, and the protein lysates were resolved by 12% SDS-PAGE. Proteins were transferred to PVDF membranes and analyzed via Western blot probing for PARP (116 kDa) and β-tubulin (55 kDa). Cleaved PARP, indicated on the blots as an 89-kDa band, is an indicator of apoptosis. *B*, HeLa cells were treated with DMSO or 25 μM TBB, DMAT, or TBBz for 12 h; proteins were then purified by TRIzol extraction and run on 7-cm pI 4–7 IPG strips for the first dimension of isoelectric focusing. Focused proteins were then run on 12% SDS-polyacrylamide gels for the second dimension followed by SYPRO Ruby protein staining. Sections from representative 2D gels are shown to illustrate changes in spot patterns between treatments. Spots 1, 2, and 3 were identified by MALDI MS as Vimentin (molecular mass, 53.7 kDa; pI 5.06) caspase cleavage products; spot 4 was identified as a Keratin 18 (molecular mass, 48.06 kDa; pI 5.34) caspase cleavage product.

Using Inhibitor-resistant CK2 Mutants to Test Drug Specificity

Validation of CK2 as an Inhibitor Target in Cells—The potency of a number of CK2 inhibitors to induce apoptosis in various cancer cells raises promising avenues for targeting CK2 for anti-cancer therapeutics. Studies performed *in vitro* utilizing CK2 inhibitors have demonstrated their high effectiveness at inhibiting CK2 kinase activity. However, the specificity and mechanism of action of these ATP-competitive inhibitors have not been systematically explored in an unbiased manner. To investigate the ability of TBB, TBBz, and DMAT to inhibit CK2 activity in cells, the autophosphorylation of CK2β by CK2α/α' was examined. The autophosphorylation of CK2β has been shown to be essential for its stability and to be a marker of assembly of CK2 tetrameric complexes. Therefore, autophosphorylated CK2β exists predominantly in complex with CK2α/α' in the phosphorylated form (27–30). *In vitro* studies testing the effectiveness of CK2 inhibitor-resistant mutants have been performed and demonstrated that the mutants are fully functional and resistant to TBB, TBBz, and DMAT (17, 24).

To extend the analysis of the inhibitors and to validate drug specificity, HeLa cells co-expressing wild type CK2α-HA or resistant CK2αR-HA in addition to myc-CK2β6KR (Mycβ) were treated with either 8 μM TBBz, DMAT, or TBB as well as DMSO as a control for 18 h (Fig. 3). The proteasome-resistant myc-CK2β6KR mutant was used to investigate CK2 tetrameric complex formation (31). Wild type CK2α and resistant CK2αR were immunoprecipitated from treated cells, and the levels of complexed Mycβ-P_i were analyzed. Consistent with previous findings, treatment of cells expressing wild type CK2 in the presence of the CK2 inhibitors resulted in the reduction of CK2α-Mycβ-P_i complex formation as compared with treatment with the drug carrier DMSO as was evident by the reduced CK2α and Mycβ-P_i levels. Interestingly the expression of the inhibitor-resistant CK2 rescued the loss of CK2α-Mycβ-P_i complex formation as was evident by stable formation of CK2α-Mycβ-P_i complexes and increased CK2α and Mycβ-P_i levels. Overall introduction of the inhibitor-resistant CK2αR rescued the reduction of CK2α and Mycβ-P_i levels in the tetrameric complex, indicating that restoration of CK2α kinase activity was capable of autophosphorylating CK2β,

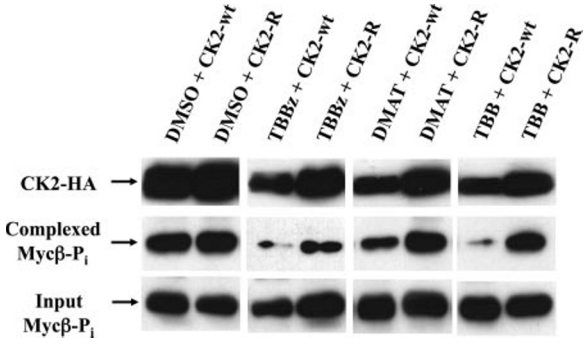

FIG. 3. **Using inhibitor-resistant CK2 mutants to test drug specificity.** Rescue of CK2β autophosphorylation following treatment with CK2 inhibitors using inhibitor-resistant CK2 mutants was demonstrated in HeLa cells co-transfected with CK2α-HA or CK2αR-HA in addition to myc-CK2β6KR (Mycβ) and EGFP-C2 at a transfection efficiency of >80%. Cells were treated with DMSO or 8 μM TBBz, DMAT, or TBB for 18 h. CK2α-HA and CK2αR-HA were immunoprecipitated from lysates and run on a 12% SDS-polyacrylamide gel followed by transfer to a PVDF membrane. A decrease in the formation of tetrameric complexes as well as complexed Mycβ-P$_i$ in the presence of TBBz, DMAT, and TBB was indicated by the reduction of the 32.5-kDa Mycβ-P$_i$ band and the 50-kDa CK2α-HA band as shown via Western blot analysis by probing membranes with anti-Myc 9E10 and anti-HA 3F10 antibodies compared with the control DMSO. The rescue of the formation of CK2 tetrameric complexes and loss of Mycβ-P$_i$ in the presence of the inhibitors was demonstrated by restoring the 50-kDa CK2α-HA and the 32.5-kDa Mycβ-P$_i$ bands back to DMSO levels. The levels of Mycβ-P$_i$ in cells prior to immunoprecipitations are shown by Western blot analysis as a control.

thus stabilizing CK2α-CK2β complex formation. Inhibitor-resistant CK2α' (V67A/I175A) mutants were also shown to be capable of forming functional tetrameric complexes as well as being proficient at restoring the loss of autophosphorylation of Mycβ associated with inhibitor treatment (supplemental material).

Overall the treatment of cells with CK2 inhibitors TBB, TBBz, and DMAT resulted in the inhibition of autophosphorylation of CK2β by CK2α/α'. The rescue of the autophosphorylation of CK2β by CK2αR/α'R validates that the inhibitors reduce CK2 kinase activity in cells that can be restored by expression of resistant CK2.

Inhibitor-resistant Mutants Are Unable to Rescue Apoptosis—A number of inhibitors of CK2 including TBB, TBBz, and DMAT have all been shown to negatively affect the viability of various cancer cell lines (19, 24, 32). This was also observed in the present study in which treatment of HeLa cells with TBBz, DMAT, and to a lesser extent TBB induced apoptosis in a concentration- and duration-dependent manner. In rescue experiments, it was shown that TBB, TBBz, and DMAT inhibited the autophosphorylation of CK2β in cells that could be restored by expressing inhibitor-resistant CK2 mutants.

To test whether the apoptotic response associated with TBB, DMAT, and TBBz was due to inhibition of CK2 activity, rescue experiments utilizing inhibitor-resistant CK2 were carried out. HeLa cells expressing CK2αR and CK2α'R were treated with DMSO or 8 μM TBB, DMAT, or TBBz for 18 h, and apoptosis was determined by assaying for cleaved PARP by Western blot (Fig. 4*A*) and by calculating the percentage of cells in the sub-G_0/G_1 population via FACS (Fig. 4*B*). Interestingly cells expressing the inhibitor-resistant forms of CK2 still showed evidence of apoptosis following treatment with TBBz or DMAT, as indicated by the presence of cleaved PARP as well as a large percentage of cells in the sub-G_0/G_1 population, compared with DMSO controls. By comparison no apoptosis was observed in TBB-treated cells either with or without expression of resistant CK2. Overall this evidence suggests that the apoptosis associated with TBBz and DMAT was not exclusively due to loss of CK2 activity as restoration via expression of inhibitor-resistant mutants was not capable of rescuing cells from apoptosis. Interestingly treatment of cells with 8 μM TBB resulted in a reduction of CK2 activity as was evident by the loss of CK2β autophosphorylation but no induction of apoptosis.

The potency of TBBz and DMAT in inducing a CK2-independent apoptosis, even at low drug concentrations, raises the possibility of off-target drug effects and cytotoxicity. In this respect, evidence presented here suggests that the death associated with TBBz and DMAT may not be attributed solely to the inhibition of CK2 but rather the inhibition of other ATP-binding proteins that are essential for cell viability.

Identification of Novel Inhibitor Interactors: Evidence for Off-target Effects

Confirmation of CK2 as a Bona Fide Target of TBB and Its Derivatives—To validate CK2 as an inhibitor target, a chemoproteomics strategy was used. Accordingly a proteomics approach using ATP-Sepharose affinity chromatography was performed to test the specificity of TBB, TBBz, and DMAT for CK2. An inhibitor competition assay was performed, consisting of preincubation of HeLa S3 cell lysates with DMSO or 100 μM TBB, DMAT, or TBBz followed by the addition of ATP-Sepharose beads. If the inhibitor interacted with an ATP-binding protein with strong affinity it would prevent that protein from binding to the ATP-Sepharose. To test whether CK2 was a *bona fide* target of TBB, DMAT, or TBBz among all cellular ATP-binding proteins, a comparative analysis of the proteins bound to the ATP-Sepharose beads following inhibitor treatment was performed via Western blot analysis for CK2α and CK2α' (Fig. 5*A*). Incubation of HeLa cell lysates with 100 μM TBB, DMAT, or TBBz prevented CK2α and CK2α' from binding to the ATP-Sepharose relative to the control DMSO levels. Interestingly the reduction in CK2α' immunoreactivity observed in the presence of 100 μM TBBz could be restored to control levels by reducing the inhibitor concentration to 1 μM, indicating a concentration-dependent competition (supplemental material). HSP90 was used as a loading control, which was unaffected by the inhibitor competition

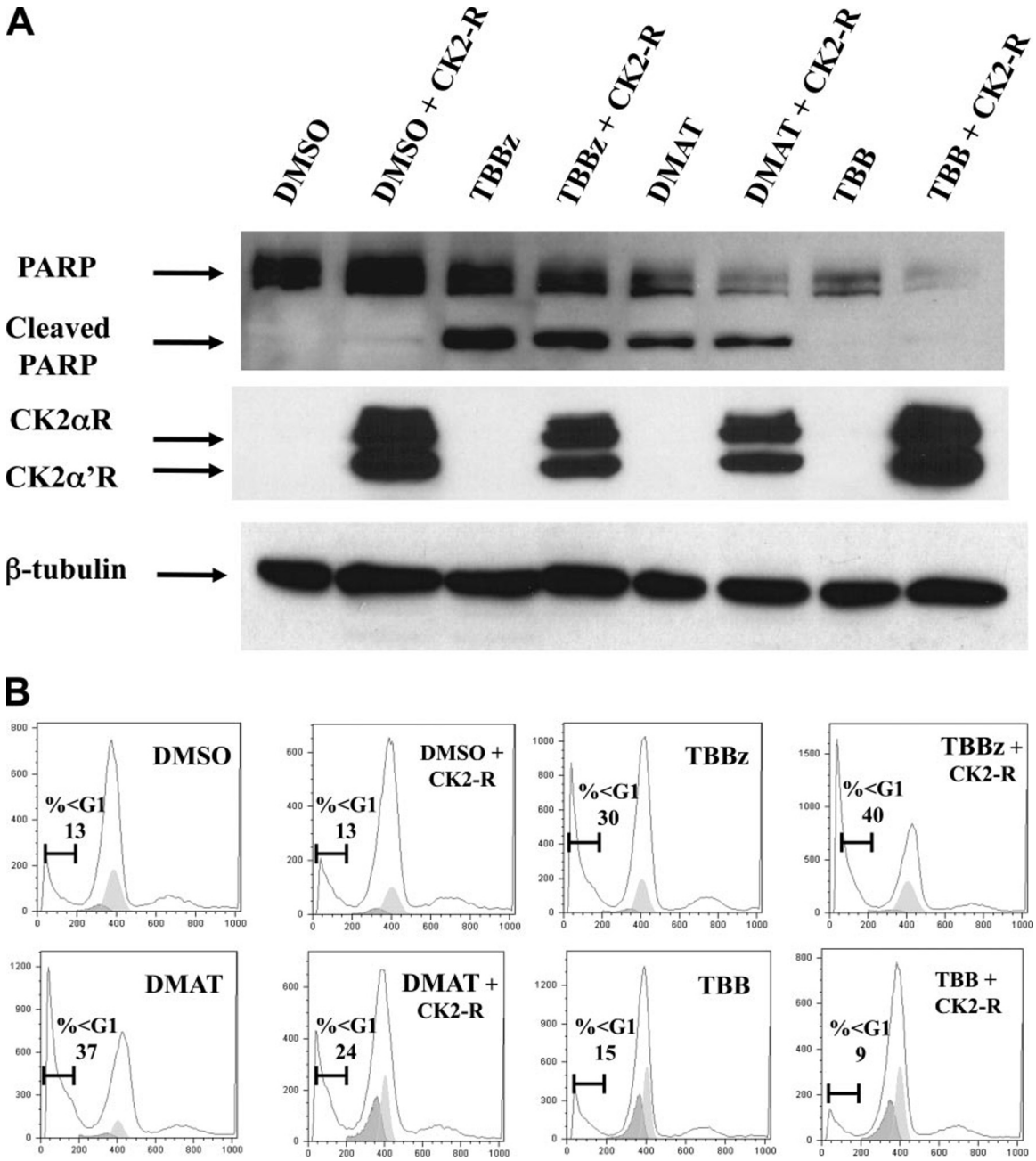

FIG. 4. **Apoptosis associated with TBBz and DMAT treatment was independent of CK2 activity.** *A*, TBBz- and DMAT-induced apoptosis could not be rescued by restoring CK2 activity in cells. HeLa cells were co-transfected with CK2αR-HA/HA-CK2α′R along with myc-CK2β6KR and EGFP-C2 at a transfection efficiency of >80% and treated with either DMSO or 8 μM TBBz, DMAT, or TBB for 18 h. Apoptosis was determined by the presence of the 89-kDa cleaved PARP band in TBBz- and DMAT-treated cells expressing inhibitor-resistant CK2 mutants compared with DMSO. No cleavage of PARP was detected in cells treated with TBB. Confirmation of expression of resistant mutants was determined by the presence of 50-kDa CK2αR-HA and 40-kDa HA-CK2α′R bands. Western blot analysis was performed using anti-PARP, anti-HA 3F10, and anti-β-tubulin antibodies. *B*, inhibitor-induced apoptosis in HeLa cells co-transfected with CK2αR-HA/HA-CK2α′R along with myc-CK2β6KR was assayed by FACS via the determination of the percentage of cells in the sub-G_0/G_1 population. FACS samples were prepared as described earlier. A reduction in the percentage of cells in the sub-G_0/G_1 population of apoptosis was not observed in cells expressing resistant CK2 following treatment with 8 μM TBB, DMAT, or TBBz.

assay. Taken together, CK2α and CK2α′ were found to interact with TBB, DMAT, and TBBz among all other ATP-binding proteins, further validating CK2 as a *bona fide* target of TBB and its derivatives.

Identification of Novel TBBz and DMAT Off-targets—Following the validation of CK2 as a target of the TBB-related compounds, a more global analysis of inhibitor protein interactors was explored utilizing the chemoproteomics ap-

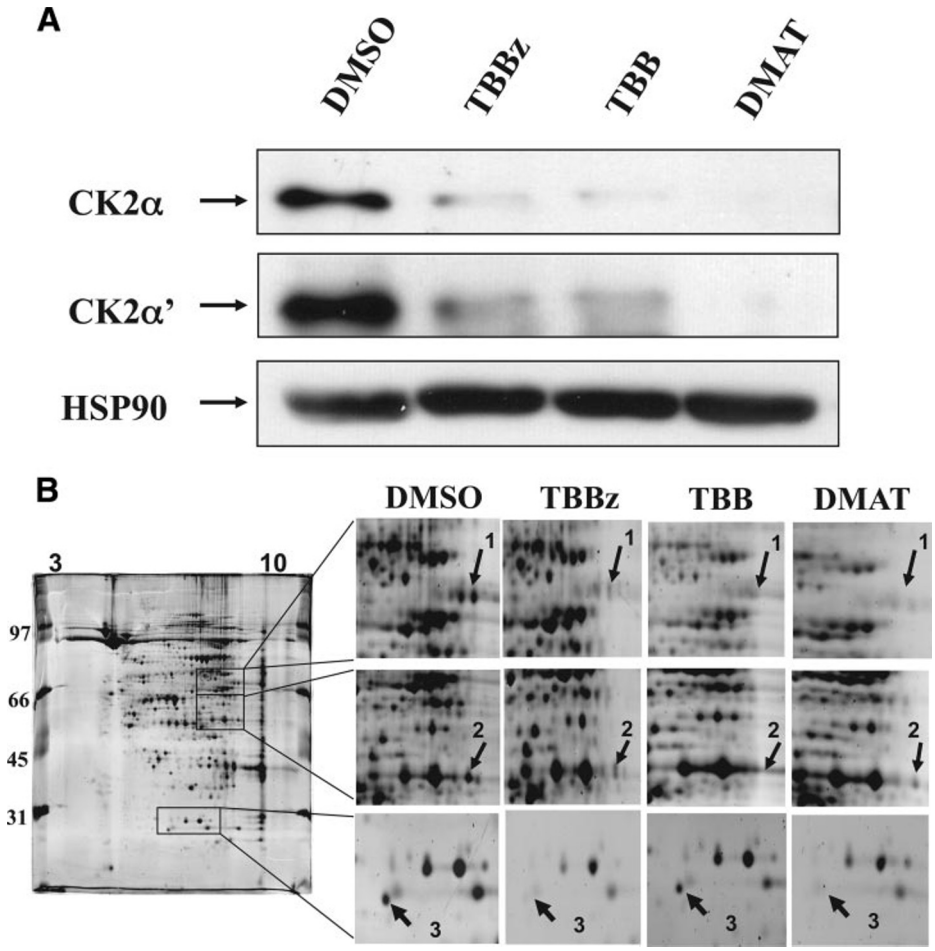

FIG. 5. **Exploiting an unbiased chemoproteomics approach to identify CK2 inhibitor interactions.** *A*, CK2α and CK2α' were shown to be targets of TBB, TBBz, and DMAT. HeLa S3 cells were harvested in buffer A (see "Materials and Methods") and incubated with DMSO or 100 μM TBBz, DMAT or TBB. An inhibitor competition assay was then performed followed by Western blot analysis by probing blots with anti-CK2α', anti-CK2α, and anti-HSP90 antibodies. The decrease in the 48-kDa CK2α band and 38 kDa CK2α' band upon inhibitor treatment indicated a competition for ATP binding, suggesting that TBBz, TBB, and DMAT all interacted with CK2 compared with the DMSO control. *B*, a number of spot changes were observed upon CK2 inhibitor treatment, indicating a number of putative CK2-inhibitor interactions. HeLa S3 cells were harvested in buffer A (see "Materials and Methods") and incubated with 100 μM DMSO, TBBz, DMAT, or TBB. An inhibitor competition assay was then performed by the addition of ATP-Sepharose beads to preinhibitor-treated lysates. Following extensive bead washes, proteins were isolated and analyzed by 2D gel electrophoresis. 2D gels were then stained with SYPRO Ruby and analyzed for spot differences with Phoretix 2D Evolution software. *Enlarged sections* from representative 2D gels from DMSO-, TBB-, TBBz-, and DMAT-treated lysates illustrate differences in spot patterns. The presence of protein spots on the DMSO gels and not on the inhibitor gels were compared, and putative inhibitor interactions were identified and labeled as spots 1–3 on gels. Proteins identified as corresponding to inhibitor-dependent spot changes are listed in Table I.

proach. The inhibitor competition assay, as described earlier, was used in combination with 2D gel electrophoresis and mass spectrometry to identify potential drug off-targets. A comparison of the proteins bound to the ATP-Sepharose beads was performed utilizing 2D gel electrophoresis, and the protein patterns were analyzed using 2D Phoretix software. A number of putative inhibitor drug targets were identified by mass spectrometry as being present on the DMSO control gels and absent on the CK2 inhibitor-treated gels (spots 1–3) (Fig. 5*B*), including caseinolytic peptidase B (HSP78), multifunctional protein ADE2, and the detoxifying protein quinone reductase 2 (QR2) (supplemental Tables 1 and 2). QR2 (spot 3) was identified as being present in the DMSO- and TBB-treated gels but not in the TBBz- and DMAT-treated gels (Fig. 6*A*). This suggests that an inhibitor competition occurred, providing evidence for a novel TBBz and DMAT drug target. The spot intensity values were analyzed by ANOVA to determine statistical significant differences ($p = 0.003$), and treatment means were compared using a *t* test (Fig. 6*B*). Spot 3 (QR2) from the DMSO and TBB gels was subjected to MALDI MS analysis, which produced a prominent peak with a m/z value of 1986.10 (Fig. 6*C*). MALDI MS/MS was carried out on the 1986.10 peptide to obtain protein sequence data (Fig. 6*D*). The tryp-

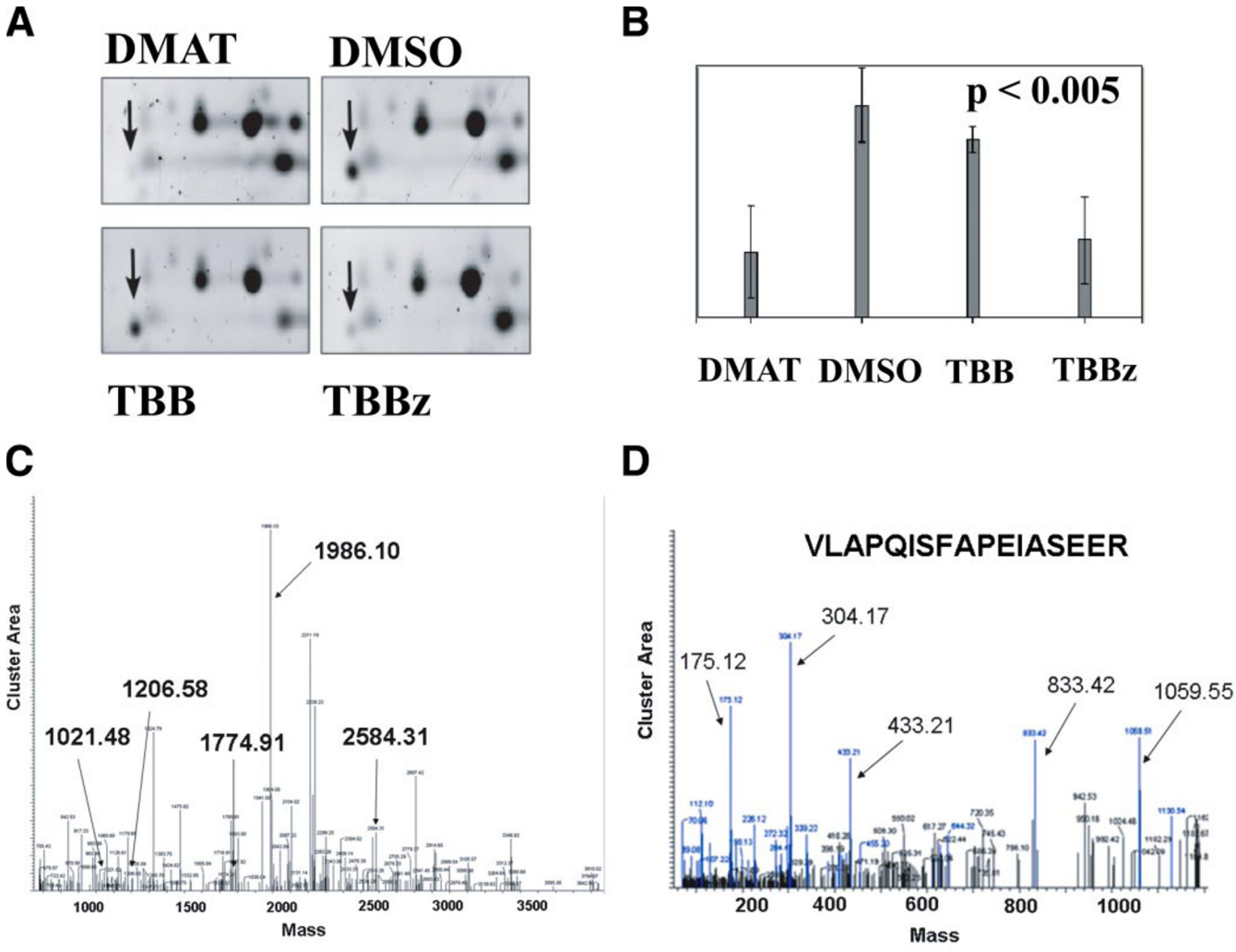

E **Peptide match summary for Quinone Reductase 2 (QR2)**

1	MAGKKVLIVY	AHQEPKSFNG	SLKNVAVDEL	SRQGCTVTVS	DLYAMNLEPR
51	ATDKDITGTL	SNPEVFNYGV	ETHEAYKQRS	LASDITDEQK	KVREADLVIF
101	QFPLYWFSVP	AILKGWMDRV	LCQGFAFDIP	GFYDSGLLQG	KLALLSVTTG
151	GTAEMYTKTG	VNGDSRYFLW	PLQHGTLHFC	GFKVLAPQIS	FAPEIASEEE
201	RKGMVAAWSQ	RLQTIWKEEP	IPCTAHWHFG	Q	

FIG. 6. **Identification of a novel TBBz and DMAT off-target, quinone reductase 2.** *A*, enlarged representation of spot 3 (QR2) identified from the 2D gels shown in Fig. 5*B*. The absence of QR2 from TBBz- and DMAT-treated gels indicates that the CK2 inhibitors prevented QR2 from binding to ATP-Sepharose, indicating an inhibitor-QR2 interaction. *B*, a statistical difference in QR2 binding to ATP-Sepharose between DMSO, TBB, TBBz, and DMAT was determined by comparing 2D gel spots using ANOVA ($p = 0.003$), and comparison of treatment means was done by *t* test at $p = 0.05$. *C*, representative MALDI MS spectrum of trypsin-digested peptides picked from spot 3 and corresponding to QR2 (molecular weight, 25,936; pI 5.88). *D*, MS/MS spectrum of the 1986.10-Da peptide fragment derived from QR2 (spot 3). *E*, peptide match summary for QR2 as identified by MASCOT. Matched peptides and 46% sequence coverage are highlighted in *red*.

sin peptide fragments were analyzed by MASCOT, and QR2 (molecular mass, 25.6 kDa; pI 5.88) was identified with a sequence coverage of 46% (Fig. 6*E*). The use of a chemoproteomics strategy to identify TBB, TBBz, and DMAT protein targets revealed that CK2 is a target for the inhibitors; however, discovery of novel metabolic targets that interact

TABLE I
Identification of putative off-target CK2 inhibitor interactions
Proteins were identified by MALDI MS or MALDI MS/MS. Spots 1–3 were identified on 2D gels depicted in Fig. 5*B*.

Spot no.	Protein	Inhibitor interactor	Accession number	Calculated mass	Observed mass	Calculated pI	Observed pI
				kDa	*kDa*		
1	Caseinolytic peptidase B (HSP78)[a]	TBB TBBz DMAT	Q9H078	78.6	79	9.13	9.0
2	Multifunctional protein (ADE2)[a]	TBB TBBz DMAT	P22234	47.1	52	6.95	8.8
3	QR2[b]	TBBz DMAT	P16083	25.9	30	5.88	6.0

[a] Protein identification by MALDI-TOF mass spectrometry.
[b] Protein identification by MALDI-TOF/TOF mass spectrometry.

strongly with TBBz and DMAT raises the issue of the specificity of these CK2 inhibitors.

DISCUSSION

The role of CK2 in the progression of tumorigenesis has become increasingly evident as the dysregulation of a number of pathways has been attributed to abnormally high levels of CK2 activity. Consequently preclinical studies investigating CK2 as a molecular therapeutic target have been ongoing, resulting in the development of various ATP-competitive inhibitors including the structurally related compounds TBB, TBBz, and DMAT (Fig. 1). However, the molecular mechanism by which these chemicals function in cells has not been systematically explored.

An unbiased characterization of available CK2 inhibitors was undertaken to investigate CK2 as a pharmacological anticancer target as well as to explore the potential of the inhibitors to study CK2 function. The inhibitors displayed varying abilities to induce apoptosis in cells suggesting a distinct mechanism of action. Validation of the ability of the inhibitor to reduce CK2 activity in cells was demonstrated by the loss of autophosphorylation of CK2β by CK2α/α' that was then restored in cells expressing inhibitor-resistant CK2 mutants. Rescue experiments addressing inhibitor specificity were carried out and determined that the apoptosis observed following DMAT and TBBz treatment could not be rescued by reintroduction of functional CK2. To validate CK2 as an inhibitor target, a chemoproteomics approach was carried out that determined that CK2α and CK2α' were indeed TBB, TBBz, and DMAT targets. Significantly a number of putative off-target drug interactions were identified, including a novel TBBz and DMAT target, QR2. The discovery of QR2 as a putative CK2 inhibitor drug target provides possible explanations for the toxic effects associated with the inhibitors as well as raises the prospect of a new therapeutic potential for TBBz and DMAT in other diseases. The unbiased evaluation of CK2 inhibitors provides evidence that TBBz and DMAT have potential off-target effects; however, due to the prominent role of CK2 in tumorigenesis, inhibition of this kinase remains a promising anticancer therapeutic avenue.

The classical method for addressing kinase inhibitor specificity has been the use of panel screens in which a number of kinases from different families are tested for an inhibitory effect (3). The limitation to this strategy has become evident as the screens are not comprehensive and fail to consider the presence of other ATP-binding proteins, including key metabolic and regulatory proteins. The chemoproteomics approach comprises an unbiased identification of drug-binding proteins through ATP affinity purification in conjunction with proteomics and mass spectrometry (33). A chemoproteomics approach revealed that the CK2 inhibitors prevented CK2α and CK2α' from binding to ATP-Sepharose in a concentration-dependent manner, reiterating that CK2 was a target of TBB, TBBz, and DMAT. Significantly the observation that 1 μM TBBz was not a sufficient concentration to inhibit CK2α' from binding to the ATP-Sepharose but was, however, an adequate concentration to induce apoptosis in HeLa cells suggested that the apoptosis was not due to the inhibition of CK2. Therefore, further analysis was performed to identify off-target protein-inhibitor interactions that could provide an explanation for the inability of inhibitor-resistant CK2 mutants to rescue the apoptosis associated with TBBz and DMAT. An analysis of the ATP-binding proteins treated with CK2 inhibitors revealed a number of interesting proteins involved in cell survival, metabolism, and drug detoxification (Table I).

Competition of QR2 from binding to ATP-Sepharose was observed with TBBz and DMAT but not TBB, indicating drug target differences between inhibitor derivatives. QR2 has a role in the detoxification processes of quinones, specifically the two-electron reduction of menadione by the oxidation of *N*-alkylated or *N*-ribosylated nicotinamides (34). Knock-out models of QR2 in mice result in an increased susceptibility to polycyclic aromatic hydrocarbon-induced skin carcinogenesis, whereas inhibition of QR2 using quinacrine resulted in

death of malaria-infected red blood cells by altering the redox status of the cell (33, 35). Recently a role for QR2 in the tumor necrosis factor apoptotic signaling pathway has emerged in which QR2-deficient keratinocytes were shown to have suppressed survival signals and increased tumor necrosis factor-induced apoptosis (36). Intriguingly other studies investigating the mechanism of action of Abelson protein tyrosine kinase and protein kinase C kinase inhibitors demonstrated QR2 as a nonkinase novel drug target, suggesting a potential role for QR2 in the drug metabolism (37–39). In the present study, the discovery of QR2 as a novel TBBz and DMAT drug target provides opportunities to further explore the mechanism by which cell viability is affected following treatment with CK2 inhibitors. Interestingly quercetin, a flavanoid and known inhibitor of CK2 with an $IC_{50} = 0.55\ \mu M$, has also been described as a potent competitive inhibitor of QR2 with a K_i of 0.021 μM (40, 41). The crystal structure of QR2 with the inhibitor resveratrol has been solved and showed that the active binding site was composed of a very hydrophobic cavity favoring the binding of flat planar conformations (40). The hydrophobic cavity of QR2 could facilitate the binding of CK2 inhibitors that were designed to maximize hydrophobic interactions with the large bulky side chains within the CK2 ATP binding pocket. The evolution of TBB to generate higher affinity inhibitors for CK2 resulted in an imidazole ring substitution as well as the addition of bulky constituents to facilitate the interaction with the hydrophobic pocket of CK2 (19). One could envisage the strong hydrophobic binding properties and planar structure of TBBz and DMAT binding into the QR2 hydrophobic cavity, potentially altering or inhibiting its ability to function. Previous studies have shown that QR2 has the potential to activate CB1954 prodrug into a highly toxic DNA-damaging agent, indicating the possibility that TBBz and DMAT could be modified (42). The inability of TBB to bind to QR2 offers an explanation as to why TBBz and DMAT are more potent at inducing apoptosis. TBBz and DMAT could bind to QR2 and either inhibit the function of the protein leading to alterations in redox levels or could potentially be modified by QR2 into more cytotoxic compounds facilitating an off-target response. However, further inhibitory studies are required to test the efficacy of TBBz and DMAT to inhibit QR2 *in vitro* as well as *in vivo*. It will be of interest to determine the efficiency of TBBz and DMAT to inhibit QR2 as they might prove useful in the study of other diseases such as malaria.

The use of the inhibitors to study the role of CK2 in physiological processes will require caution and the use of rescue experiments to validate the CK2-dependent phenotypes. The identification of a number of putative metabolic off-targets provides evidence that the study of ATP-competitive inhibitors such as CK2 inhibitors will require vigorous testing to validate the specificity of the inhibitors in cells. Further the relative abundance of the proposed drug target within various cells will also be essential in determining the specificity of inhibitors. Other cellular targets that are less sensitive to the inhibitors may be affected or inhibited by the drugs due to higher abundance than that of the proposed target. Therefore, other strategies to inhibit CK2 may be required to maximize selectivity, including identifying compounds that inhibit CK2 via allosteric interaction, independent of the ATP-binding site. The production of peptide inhibitors specific for CK2 has been a promising avenue of research as a number of groups have successfully developed and characterized the inhibition of CK2 in cells. Inhibition of CK2 using a CK2-specific peptide resulted in the reduction of CK2 activity and of tumor growth in a mouse model, reiterating CK2 as a promising drug target (43).

Acknowledgments—We thank Dr. Ken Yeung and Christina Jurcic for use of the MALDI/Mass Spectrometry Facility within the Schulich School of Medicine and Dentistry at the University of Western Ontario as well as for helpful input into the analysis of mass spectra. We also thank Cunjie Zhang and Christopher Ward from the Functional Proteomics Facility at the University of Western Ontario for help in the digestion and preparation of mass spectrometry samples as well as for guidance in the analysis of 2D gel spot patterns.

* This work was supported in part by Canadian Institute of Health Research Grant MOP 37854 and National Cancer Institute of Canada Grant 13213 with funds from the Canadian Cancer Society. The costs of publication of this article were defrayed in part by the payment of page charges. This article must therefore be hereby marked "*advertisement*" in accordance with 18 U.S.C. Section 1734 solely to indicate this fact.

[S] The on-line version of this article (available at http://www.mcponline.org) contains supplemental material.

§ Jointly supported by a Canadian Institute of Health Research-Canadian Graduate Scholarship, Canadian Institute of Health Research-University of Western Ontario Strategic Training Initiative in Cancer Research and Technology Transfer scholarship, and Ontario Graduate Scholarship.

‖ Supported by Polish Ministry of Science and Higher Education Grant PBZ-MIN 014/P05/2004.

§§ To whom correspondence should be addressed. Tel.: 519-661-4186; Fax: 519-661-3175; E-mail: litchfi@uwo.ca.

REFERENCES

1. Jabbour, E., Cortes, J. E., Giles, F. J., O'Brien, S., and Kantarjian, H. M. (2007) Current and emerging treatment options in chronic myeloid leukemia. *Cancer* **109,** 2171–2181
2. Hopkins, A. L., and Groom, C. R. (2002) The druggable genome. *Nat. Rev. Drug Discov.* **1,** 727–730
3. Pagano, M. A., Cesaro, L., Meggio, F., and Pinna, L. A. (2006) Protein kinase CK2: a newcomer in the 'druggable kinome'. *Biochem. Soc. Trans.* **34,** 1303–1306
4. Litchfield, D. W. (2003) Protein kinase CK2: structure, regulation and role in cellular decisions of life and death. *Biochem. J.* **369,** 1–15
5. Faust, R. A., Tawfic, S., Davis, A. T., Bubash, K., and Ahmed, K. (2000) Antisense oligonucleotides against protein kinase CK2-α inhibit growth of squamous cell carcinoma of the head and neck in vitro. *Head Neck* **22,** 341–346
6. Daya-Makin, M., Sanghera, J. S., Mogentale, T., Lipp, M., Parchomchuk, J., Hogg, J., and Pelech, S. (1994) Activation of a tumour-associated protein kinase (p40TAK) and casein kinase II in human squamous cell carcinomas and adenocarcinomas of the lung. *Cancer Res.* **54,** 2262–2268
7. Landesman-Bollag, E., Romieu-Mourez, R., Song, D. H., Sonenshein, G. E., Cardiff, R. D., and Seldin, D. C. (2001) Protein kinase CK2 in mammary gland tumorigenesis. *Oncogene* **20,** 3247–3257
8. Song, D. H., Dominguez, I., Mizuno, J., Kaut, M., Mohr, S. C., and Seldin, D. C. (2003) CK2 phosphorylation of the armadillo repeat region of

β-catenin potentiates Wnt signaling. *J. Biol. Chem.* **278,** 24018–24025
9. Barroga, C. F., Stevenson, J. F., Schwarz, E. M., and Verma, I. M. (1995) Constitutive phosphorylation of I kappa B alpha by casein kinase II. *Proc. Natl. Acad. Sci. U. S. A.* **92,** 7637–7641
10. Di Maira, G., Salvi, M., Arrigoni, G., Marin, O., Sarno, S., Brustolon, F., Pinna, L. A., and Ruzzene, M. (2005) Protein kinase CK2 phosphorylates and upregulates Akt/PKB. *Cell Death Differ.* **12,** 668–677
11. Duncan, J. S., and Litchfield, D. W. (2008) Too much of a good thing: the role of protein kinase CK2 in tumorigenesis and prospects for therapeutic inhibition of CK2. *Biochim. Biophys. Acta* **1784,** 33–47
12. Desagher, S., Osen-Sand, A., Montessuit, S., Magnenat, E., Vilbois, F., Hochmann, A., Journot, L., Antonsson, B., and Martinou, J.-C. (2001) Phosphorylation of Bid by casein kinases I and II regulates its cleavage by caspase 8. *Mol. Cell* **8,** 601–611
13. Krippner-Heidenreich, A., Talanian, R. V., Sekul, R., Kraft, R., Thole, H., Ottleben, H., and Luscher, B. (2001) Targeting of the transcription factor Max during apoptosis: phosphorylation-regulated cleavage by caspase-5 at an unusual glutamic acid residue in position P1. *Biochem. J.* **358,** 705–715
14. Ruzzene, M., Penzo, D., and Pinna, L. A. (2002) Protein kinase CK2 inhibitor 4,5,6,7-tetrabromobenzotriazole (TBB) induces apoptosis and caspase-dependent degradation of haematopoietic lineage cell-specific protein 1 (HS1) in Jurkat cells. *Biochem. J.* **364,** 41–47
15. Walter, J., Schindzielorz, A., Grunberg, J., and Haass, C. (1999) Phosphorylation of presenilin-2 regulates its cleavage by caspases and retards progression of apoptosis. *Proc. Natl. Acad. Sci. U. S. A.* **96,** 1391–1396
16. Yin, X., Gu, S., and Jiang, J. X. (2001) The development-associated cleavage of lens connexin 45.6 by caspase-3-like protease is regulated by casein kinase II-mediated phosphorylation. *J. Biol. Chem.* **276,** 34567–34572
17. Sarno, S., Ruzzene, M., Frascella, P., Pagano, M. A., Meggio, F., Zambon, A., Mazzorana, M., Maira, G. D., Lucchini, V., and Pinna, L. A. (2005) Development and exploitation of CK2 inhibitors. *Mol. Cell. Biochem.* **274,** 69–76
18. Pagano, M. A., Andrzejewska, M., Ruzzene, M., Sarno, S., Cesaro, L., Bain, J., Elliott, M., Meggio, F., Kazimierczuk, Z., and Pinna, L. A. (2004) Optimization of protein kinase CK2 inhibitors derived from 4,5,6,7-tetrabromobenzimidazole. *J. Med. Chem.* **47,** 6239–6247
19. Pagano, M. A., Meggio, F., Ruzzene, M., Andrzejewska, M., Kazimierczuk, Z., and Pinna, L. A. (2004) 2-Dimethylamino-4,5,6,7-tetrabromo-1H-benzimidazole: a novel powerful and selective inhibitor of protein kinase CK2. *Biochem. Biophys. Res. Commun.* **321,** 1040–1044
20. Zien, P., Bretner, M., Zastapilo, K., Szyszka, R., and Shugar, D. (2003) Selectivity of 4,5,6,7-tetrabromobenzimidazole as an ATP-competitive potent inhibitor of protein kinase CK2 from various sources. *Biochem. Biophys. Res. Commun.* **306,** 129–133
21. Haystead, C. M. H., Gregory, P., Sturgill, T. W., and Haystead, T. A. J. (1993) γ-Phosphate-linked ATP-Sepharose for the affinity purification of protein kinases: rapid purification to homogeneity of skeletal muscle mitogen-activated protein kinase kinase. *Eur. J. Biochem.* **214,** 459–467
22. Izeradjene, K., Douglas, L., Delaney, A., and Houghton, J. A. (2004) Influence of casein kinase II in tumor necrosis factor-related apoptosis-inducing ligand-induced apoptosis in human rhabdomyosarcoma cells. *Clin. Cancer Res.* **10,** 6650–6660
23. Izeradjene, K., Douglas, L., Delaney, A., and Houghton, J. A. (2005) Casein kinase II (CK2) enhances death-inducing signalling complex (DISC) activity in TRAIL-induced apoptosis in human colon cancer cell lines. *Oncogene* **24,** 2050–2058
24. Zien, P., Duncan, J. S., Skierski, J., Bretner, M., Litchfield, D. W., and Shugar, D. (2005) Tetrabromobenzotriazole (TBBt) and tetrabromobenzimidazole (TBBz) as selective inhibitors of protein kinase CK2: evaluation of their effects on cells and different molecular forms of human CK2. *Biochim. Biophys. Acta* **1754,** 271–280
25. Byun, Y., Chen, F., Chang, R., Trivedi, M., Green, K. J., and Cryns, V. L. (2001) Caspase cleavage of vimentin disrupts intermediate filaments and promotes apoptosis. *Cell Death Differ.* **8,** 443–450
26. Caulin, C., Salvesen, G. S., and Oshima, R. G. (1997) Caspase cleavage of keratin 18 and reorganization of intermediate filaments during epithelial cell apoptosis. *J. Cell Biol.* **138,** 1379–1394
27. Canton, D. A., Zhang, C., and Litchfield, D. W. (2001) Assembly of protein kinase CK2: investigation of complex formation between catalytic and regulatory subunits using zinc-finger-deficient mutant CK2β. *Biochem. J.* **358,** 87–94
28. Graham, K., and Litchfield, D. W. (2000) The regulatory β subunit of protein kinase CK2 mediates formation of tetrameric CK2 complexes. *J. Biol. Chem.* **7,** 5003–5010
29. Seeber, S., Issinger, O.-G., Holm, T., Kristensen, L. P., and Guerra, B. (2005) Validation of protein kinase CK2 as oncological target. *Apoptosis* **10,** 875–885
30. Zhang, C., Vilk, G., Canton, D. A., and Litchfield, D. W. (2002) Phosphorylation regulates the stability of the regulatory CK2β subunit. *Oncogene* **21,** 3754–3764
31. French, A. C., Luscher, B., and Litchfield, D. W. (2007) Development of a stabilized form of the regulatory CK2β subunit that inhibits cell proliferation. *J. Biol. Chem.* **282,** 29667–29677
32. Sarno, S., Reddy, H., Meggio, F., Ruzzene, M., Davies, S. P., Donella-Deana, A., Shugar, D., and Pinna, L. A. (2001) Selectivity of 4,5,6,7-tetrabromobenzotriazole, an ATP site-directed inhibitor of protein kinase CK2 ('casein kinase-2'). *FEBS Lett.* **496,** 44–48
33. Graves, P. R., Kwiek, J. J., Fadden, P., Ray, R., Hardeman, K., Coley, A. M., Foley, M., and Haystead, T. A. (2002) Discovery of novel targets of quinoline drugs in the human purine binding proteome. *Mol. Pharmacol.* **62,** 1364–1372
34. Vella, F., Ferry, G., Delagrange, P., and Boutin, J. A. (2005) NRH:quinone reductase 2: an enzyme of surprises and mysteries. *Biochem. Pharmacol.* **71,** 1–12
35. Kwiek, J. J., Haystead, T. A., and Rudolph, J. (2004) Kinetic mechanism of quinone oxidoreductase 2 and its inhibition by the antimalarial quinolines. *Biochemistry* **20,** 4538–4547
36. Ahn, K. S., Gong, X., Sethi, G., Chaturvedi, M. M., Jaiswal, A. K., and Aggarwal, B. B. (2007) Deficiency of NRH:quinone oxidoreductase 2 differentially regulates TNF signalling in keratinocytes: up-regulation of apoptosis correlates with down-regulation of cell survival kinases. *Cancer Res.* **67,** 10004–10011
37. Brehmer, D., Godl, K., Zech, B., Wissing, J., and Daub, H. (2004) Proteome-wide identification of cellular targets affected by bisindolylmaleimide-type protein kinase C inhibitors. *Mol. Cell. Proteomics* **3,** 490–500
38. Bantscheff, M., Eberhard, D., Abraham, Y., Bastuck, S., Boesche, M., Hobson, S., Mathieson, T., Perrin, J., Raida, M., Rau, C., Reader, V., Sweetman, G., Bauer, A., Bouwmeester, T., Hopf, C., Kruse, U., Neubauer, G., Ramsden, N., Rick, J., Kuster, B., and Drewes, G. (2007) Quantitative chemical proteomics reveals mechanisms of action of clinical ABL kinase inhibitors. *Nat. Biotechnol.* **25,** 1035–1044
39. Rix, U., Hantschel, O., Durnberger, G., Remsing Rix, L. L., Planyavsky, M., Fernbach, N. V., Kaupe, I., Bennett, K. L., Valent, P., Colinge, J., Kocher, T., and Superti-Furga, G. (2007) Chemical proteomic profiles of the BCR-ABL inhibitors imatinib, nilotinib, and dasatinib reveal novel kinase and nonkinase targets. *Blood* **110,** 4055–4063
40. Buryanovskyy, L., Fu, Y., Boyd, M., Ma, Y., Hsieh, T. C., Wu, J. M., and Zhang, Z. (2004) Crystal structure of quinone reductase 2 in complex with resveratrol. *Biochemistry* **43,** 11417–11426
41. Sarno, S., Salvi, M., Battistutta, R., Zanotti, G., and Pinna, L. A. (2005) Features and potentials of ATP-site directed CK2 inhibitors. *Biochim. Biophys. Acta* **1754,** 263–270
42. Fu, Y., Buryanovskyy, L., and Zhang, Z. (2005) Crystal structure of quinone reductase 2 in complex with cancer prodrug CB1954. *Biochem. Biophys. Res. Commun.* **336,** 332–338
43. Laudet, B., Barette, C., Dulery, V., Renaudet, O., Dumy, P., Metz, A., Prudent, R., Deshiere, A., Dideberg, O., Filhol, O., and Cochet, C. (2007) Structure-based design of small peptide inhibitors of protein kinase CK2 subunit interaction. *Biochem. J.* **408,** 363–373